Vibronic interaction as main reason of magnetic ordering in insulating manganites $R_{1-x}A_xMnO_3$

Liudmila Gonchar[1,2*], *Anatoliy* Nikiforov[2]

[1]Ural State University of Railway Transport, 620034 Yekaterinburg, Russia
[2]Ural Federal University, 620002 Yekaterinburg, Russia

Abstract. The model of orbitally dependent magnetic structure of charge ordered insulated manganites is proposed. The model is semi-phenomenological. It allows using a few parameters to describe possible magnetic structures of compounds. The experimental crystal structure of compounds also could be taken into account. The compounds $LaMnO_3$, $La_{1/2}Ca_{1/2}MnO_3$, $La_{1/3}Ca_{2/3}MnO_3$, $BiMnO_3$ are considered.

1 Introduction

The manganites compounds are interesting because of strong correlation between crystal, charge, orbital, and magnetic subsystems. The general formula of compounds under consideration is $R_{1-x}A_xMnO_3$, where R^{3+}=La^{3+} or Bi^{3+}, A^{2+}=Ca^{2+}, x=0, 1/2, 2/3. A field of correlation is a sublattice of Mn^{3+} ions. Mn^{3+} ion in octahedral oxygen neighborhood is a Jahn-Teller (JT) ion. The orbital states of Mn^{3+} ions form a regular structure, called orbital ordering (OO). In the case of non-isovalent doping, the charge carriers could be localized on Mn ions. This effect leads to charge ordering (CO). It means the regular structure of Mn^{3+}/Mn^{4+} ions. The magnetic structures (MS) of manganies are various [1–6]. There are A-type, E-type, CE-type, and F-type structures. OO is dependent upon crystal structure and charge distribution [7–11]. The interrelation between orbital and magnetic subsystems is also discussed [8–11]. In OO description, a choice of driving mechanism of cooperative ordering is discussed. The *ab initio* calculations require a complicated account of correlations [12, 13]. The most popular Kugel-Khomskii model [8] usually is used within the approximation of comparable vibronic and superexchange interaction. Nevertheless, the main vibronic term is estimated as ~1 eV [14], and the exchange parameters are ~1 meV [9, 10]. The rich set of MS makes difficult to create a uniform model. The main rules for estimation of the signs and relative values of superexchange (SE) parameters are Goodenough-Kanamory rules [1]. These rules use OO for MS explanation. The absence of precise values makes the MS description impossible for magnetically frustrated compounds such as $La_{1/3}Ca_{2/3}MnO_3$ or $BiMnO_3$. For SE parameters description, the *ab initio* calculations [12], Kugel-Khomskii model [8], orbitally-dependent phenomenological model [4, 9, 10, 17], next-nearest neighbor model [4, 7, 15], double-exchange model [7, 11] are applied. The *ab initio* calculations require preliminary assumption of MS [12, 13]. The double-exchange model is not applicable in suggestion of CO. We use previously proposed orbitally-dependent SE model [9, 10] to find possible MS for different orbital mixing within the framework of crystal symmetry. The aim of the paper is the description of orbital-magnetic correlation in insulating magnanites including frustrated cases.

2 Orbital state of Mn^{3+} ion

The ground state of Mn^{3+} ion's orbital subsystem with total spin S=2 in undistorted octahedral ligand neighborhood is ^5E multiplet. This state is twofold degenerated, thus some distortions of the neighborhood lead to removing of degeneration. We can use *e*-type orbital operators acting on many-electron eigenfunctions of ^5E ($|\theta\rangle$,$|\varepsilon\rangle$) in a linear combination as effective Hamiltonian

$$H_{eff}=\alpha_1 X_\theta+\alpha_2 X_\varepsilon, \quad (1)$$

where operators in matrix form are

$$X_\theta=\begin{pmatrix}-1 & 0\\ 0 & 1\end{pmatrix}\begin{matrix}\theta\\ \varepsilon\end{matrix}; X_\varepsilon=\begin{pmatrix}0 & 1\\ 1 & 0\end{pmatrix}\begin{matrix}\theta\\ \varepsilon\end{matrix}. \quad (2)$$

The α_1 and α_2 coefficients are mainly phenomenological and could be described by linear vibronic interaction, non-linear vibronic interaction or crystal field models [9, 10]. Taking into account the effective interaction (1), the ground state function is considered as a linear combination of ^5E eigenfunctions:

$$\Psi=C_1|\theta\rangle+C_2|\varepsilon\rangle, \quad (3)$$

where $C_1^2+C_2^2=1$.

More convenient are polar coordinates:

$$\alpha_1=\rho\cos\Theta,\ \alpha_2=\rho\sin\Theta,\ \Theta\in[0;2\pi). \quad (4)$$

Thus, the ground state energy and the energy gap are

$$E=-\rho,\ \Delta E=2\rho. \quad (5)$$

The ground state wave function is

* Corresponding author: l.e.gonchar@urfu.ru

$$\Psi = \left|\cos\frac{\Theta}{2}\right|\theta\rangle \pm \left|\sin\frac{\Theta}{2}\right|\varepsilon\rangle, \qquad (6)$$

where "+" is for $\alpha_2<0$, and visa versa. For magnetic properties prediction, the mean values of *X*-operators are needed.

$$\langle X_\theta\rangle = -\cos\Theta; \langle X_e\rangle = -\sin\Theta \qquad (7)$$

In the crystal, there is a sublattice of Mn ions. The orbital wave functions and orbital operators must be indexed by Mn^{3+} ion number. Thus, there are two sets of orbital interaction characteristics for n^{th} Mn^{3+} ion: 1) $\alpha_{1,n}$ and $\alpha_{2,n}$; 2) ρ_n, Θ_n. For orbital state wave function (6) only one of characteristics– Θ_n –is sufficient.

3 Superexchange interaction

The exchange interaction of two Mn ions in octahedral neighborhood could be described by general expression

$$H_{ex} = \sum_{i>j} \hat{J}_{ij}\left(\mathbf{S}_i \cdot \mathbf{S}_j\right), \qquad (8)$$

where SE operators are dependent upon orbital operators (2) of interacting ions:

$$\hat{J}_{ij} = \hat{J}_{ij}\left(X^i_\theta, X^i_\varepsilon, X^j_\theta, X^j_\varepsilon\right) \qquad (9)$$

Let us review the different kinds of orbitally-dependent 180^0-SE interaction in insulating perovskite manganties. Finding the mean values of orbital operators on the orbital state wave functions (6) of interacting ions and taking into account the Mn–O– Mn bond configuration [9, 10], one could write the SE parameters in pseudoperovskite axes as a function of orbital angles (Θ_i, Θ_j), Mn–O–Mn bond angle φ_{ij} and mean Mn–O distance r_{ij}.

1) Mn^{3+}–Mn^{3+} (*x*, *y*, *z*):

$$J^z_{ij} = \frac{J^1_0 \cos^2\varphi_{ij}}{r^{10}_{ij}}\left(1-\alpha\left(\cos\Theta_i+\cos\Theta_j\right)+\beta\cos\Theta_i\cos\Theta_j\right),$$

$$J^{x,y}_{ij} = \frac{J^1_0 \cos^2\varphi_{ij}}{r^{10}_{ij}}\times$$

$$\times\left(1+\frac{\alpha}{2}\left(\cos\Theta_i \pm\sqrt{3}\sin\Theta_i+\cos\Theta_j \pm\sqrt{3}\sin\Theta_j\right)+\right.$$

$$\left.+\frac{\beta}{4}\left(\cos\Theta_i \pm\sqrt{3}\sin\Theta_i\right)\left(\cos\Theta_j \pm\sqrt{3}\sin\Theta_j\right)\right).$$

2) Mn^{3+}–Mn^{4+} (*x*, *y*, *z*):

$$J^z_{ij} = \frac{J^2_0 \cos^2\varphi_{ij}}{r^{10}_{ij}}\left(1-\alpha'\cos\Theta_i\right),$$

$$J^{x,y}_{ij} = \frac{J^2_0 \cos^2\varphi_{ij}}{r^{10}_{ij}}\left(1+\alpha'/2\left(\cos\Theta_i \pm\sqrt{3}\sin\Theta_i\right)\right).$$

3) Mn^{4+} – Mn^{4+} : $J_{ij} = \frac{J^3_0 \cos^2\varphi_{ij}}{r^{10}_{ij}}$.

The values of parameters have been found in previous paper [9]: $J_0^1=1.69\cdot10^4$ K×Å^{10}, $\alpha=1.0$, $\beta=4.5$; $J_0^2=-4.90\cdot10^3$ K×Å^{10}, $\alpha'=5.1$; $J_0^3=1.12\cdot10^3$ K×Å^{10}. Thus, we can determine the main component of magnetic interaction.

4 Results and discussion

Let us apply the theory above to certain manganite crystals. This application was performed sometimes earlier in previous papers [9, 10, 17], but using another characteristics of OO, i.e. ϕ angle instead of Θ. It helps to remove the equivalence with MS description used in Kugel-Khomskii model [8]

4.1 $LaMnO_3$

The space symmetry of the compound is *Pnma* [1]. The OO of $LaMnO_3$ (Fig. 1) is caused by vibronic interaction of Mn^{3+} ion with local distortions of oxygen octahedra. These distortions are described by symmetrized coordinates $Q_{\theta,n}$ and $Q_{\varepsilon,n}$. The coefficients of effective Hamiltonian (1) are:

$$\alpha_{1,n} = -|V_e|Q_{\theta,n}; \alpha_{2,n} = -|V_e|Q_{\varepsilon,n}, \qquad (10)$$

where $-|V_e|Q_{\theta,n}$=0.11 eV, $-|V_e|Q_{\varepsilon,n}$=±0.34 eV.

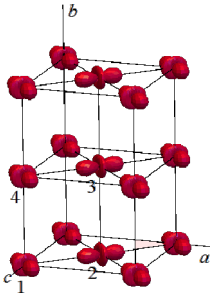

Fig.1. OO of $LaMnO_3$. Mn^{3+} ions as mixed single-electron e_g- functions are drawn. Here and on other figures, oxygen and lanthanum ions are omitted. Numbers denote Mn^{3+} ions of 4*a* position.

In terms of $\alpha_{1,n}$ and $\alpha_{2,n}$ constants, the wave function is

$$\psi_n = \left|\cos\frac{\Theta_n}{2}\right|\theta\rangle_n \pm \left|\sin\frac{\Theta_n}{2}\right|\varepsilon\rangle_n. \qquad (11)$$

All Mn^{3+} ions are divided into four sublattices due to symmetry considerations (see Fig. 1). The correlation between angles is:

$$\Theta_1 = 2\pi-\Theta_2 = 2\pi-\Theta_3 = \Theta_4 = \Theta, \Theta = 73° \qquad (12)$$

The SE interaction is of type 1. The SE dependences upon Θ angle are drawn on Fig. 2. In orthorhombic *Pnma* notations, $J_b=J^z$, $J_{ac}=J^{x,y}$.

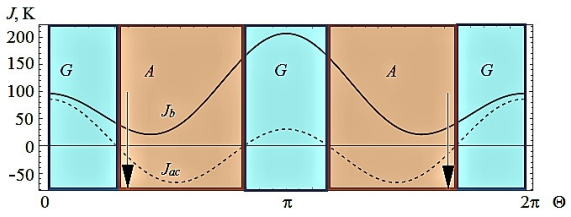

Fig. 2. Orbitally-dependent SE interaction. Arrows denote $LaMnO_3$ orbital states of Mn^{3+} ions. Letters *A* and *G* denote MS types.

As one can see at Fig. 2, the SE interaction allows only two types of AFM structure – *A* and *G*. The experimentally determined MS of $LaMnO_3$ is *A*-type AFM structure [1]. Some OO allow one-dimensional MS ($\Theta=52^0$, 149^0, 211^0, 308^0). The *G*-type MS is not observed in manganites.

4.2 $La_{1/2}Ca_{1/2}MnO_3$

The space symmetry of the compound is $P2_1/m$ [5]. At low temperature, there is CO state of the compound. The CO and OO are presented on Fig. 3.

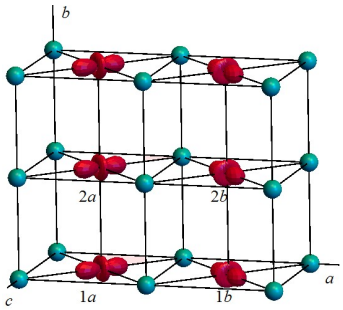

Fig.3. CO and OO of $La_{1/2}Ca_{1/2}MnO_3$. Mn^{3+} ions as mixed single-electron e_g-functions and Mn^{4+} ions as spheres are drawn. Ions of 2*a* and 2*b* positions are numbered

The OO of Mn^{3+} sublattice of $La_{1/2}Ca_{1/2}MnO_3$ is caused mainly by linear vibronic interaction of Mn^{3+} ions with local distortions of oxygen octahedra. The coefficients of vibronic Hamiltonian (1) of Mn^{3+} ions have the same form (10) as for $LaMnO_3$. The coefficients of effective Hamiltonian (1) are:

$$\alpha_{1,n} = -|V_e|Q_{\theta,n}; \alpha_{2,n} = -|V_e|Q_{\varepsilon,n}, \quad (13)$$

where $-|V_e|Q_{\theta,n}$=0.09 eV, $-|V_e|Q_{\varepsilon,a}$=–0.23 eV, $-|V_e|Q_{\varepsilon,b}$=0.21 eV.

The wave functions of the Mn^{3+} sublattice is of the same form as in Eqs. (11). The OO is described by correlation:

$$\Theta_{1a} = \Theta_{2a}\Theta_a, \Theta_{1b} = \Theta_{2b} = \Theta_b, \Theta_b \approx 2\pi - \Theta_a = 56°. \quad (14)$$

The SE interaction is of types 1–3. The second type of SE interaction defines planar interaction (J^x, J^y), and 1, 3 types are interplanar (J^z). The dependences of SE parameters upon Θ angle are drawn on Fig. 4. In monoclinic $P2_1/m$ notations, $J_b=J^z$, $J_{ac}=J^{x,y}$.SE parameter of Mn^{4+}–Mn^{4+} interaction is J=15 K [9].

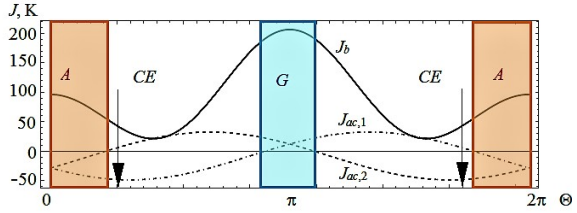

Fig. 4. Orbitally-dependent SE interaction. Arrows denote two states of Mn^{3+} sublattice in $La_{1/2}Ca_{1/2}MnO_3$. Letters *A*, *G*, and *CE* denote MS types.

The magnetic cell is described by doubled crystal cell. The changes of OO may cause the change in the MS. The experimental MS of $La_{1/2}Ca_{1/2}MnO_3$ is *CE* structure [5]. It consists of FM zigzag chains along *a* axis with AFM order between chains. The *A*-type of MS is the nearest structure on the diagram.

4.3 $La_{1/3}Ca_{2/3}MnO_3$

The space symmetry of the compound is *Pnma* [21] that is tripled compared with $LaMnO_3$. At low temperature, the CO state is also proposed [17, 18]. The CO and OO are presented on Fig. 5. The OO of Mn^{3+} sublattice of $La_{1/3}Ca_{2/3}MnO_3$ is caused mainly by vibronic interaction of Mn^{3+} ion with local distortions of oxygen octahedra. The coefficients of vibronic Hamiltonian (1) of Mn^{3+} ions have the same form (11) as for $LaMnO_3$. They must be slightly corrected, because it helps describing MS [17].

$$\alpha_{1,n} = -|V_e|Q_{\theta,n} + \alpha_{\theta,n}; \alpha_{2,n} = -|V_e|Q_{\varepsilon,n} + \alpha_{\varepsilon,n}, \quad (15)$$

where $-|V_e|Q_{\theta,n}$=0.24 eV, $-|V_e|Q_{\varepsilon,n}$=±0.31 eV.

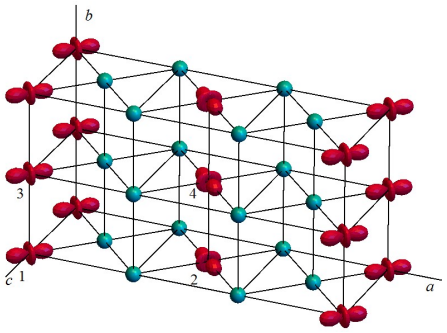

Fig. 5. CO and OO of $La_{1/3}Ca_{2/3}MnO_3$. Mn^{3+} ions as mixed single-electron e_g- functions and Mn^{4+} ions as spheres are drawn. Numbers denote Mn^{3+} ions of 4*a* position.

The wave function of the Mn^{3+} sublattice is of the same form as in Eq. (11). The OO is described by correlation:

$$\Theta_1 = 2\pi - \Theta_2 = 2\pi - \Theta_3 = \Theta_4 = \Theta, \Theta = 53° \quad (16)$$

The SE interaction is of types 1–3. The SE parameters dependent upon Θ angle are the same as in $La_{1/2}Ca_{1/2}MnO_3$ and are drawn on Fig. 4. SE parameter of Mn^{4+}–Mn^{4+} interplanar interaction is J_b=15 K [9], and J_{ac}=15 K [17] in the *ac*-plane. Taking into account the frustration of MS in Mn^{3+}–Mn^{4+} or Mn^{4+}–Mn^{4+} pairs within the *ac*-plane, one can suppose three possible types of MS. The magnetic moments in two structures form FM trimers along elongated O–Mn^{3+}–O bond. They are differently located relative to each other. The structure 1 (Fig 6a) has Mn^{3+}–Mn^{4+} FM ordered bond with AFM SE interaction. It does not double the crystal unit cell. On Fig. 6b, the FM Mn^{4+}–Mn^{3+}–Mn^{4+} trimers are ordered as stripes, which are perpendicular to each other. Fig. 6b structure has doubled crystal unit cell along *c*-axis.

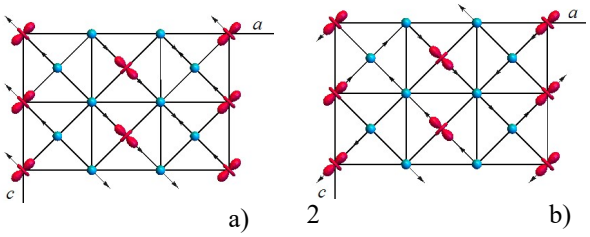

Fig. 6. Frustrated MS of 1 and 2 types of $La_{1/3}Ca_{2/3}MnO_3$ in one of *ac*-planes. In neighbor plane the spin moments are directed opposite.

The experimental investigation [18] has determined MS of type 2. However, the local oxygen octahedral distortions account in OO lead to type 1 structure. Taking into account possible terms $\alpha_{\theta,n}$, $\alpha_{\varepsilon,n}$ in vibronic interaction (15), Θ may change slightly. On Fig. 7, the region of mixing angle is drawn as wide arrows. The possible values of Θ angles supportingthe experimental MS are $\Theta \leq 305^0$, $\Theta \geq 55^0$ The additional parts of Hamiltonian's coefficients could be estimated as $|\alpha_{\theta,n}|$, $|\alpha_{\varepsilon,n}|$~0.01 eV/Å. The edge of the region is established

qualitatively, taking into account the Neel temperature of the compound.

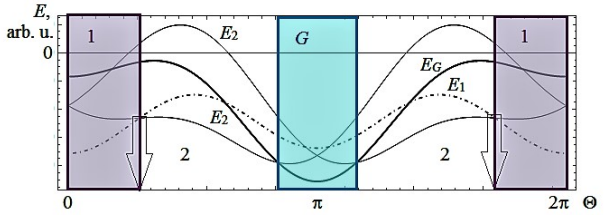

Fig. 7. Orbitally-dependent energy of possible MS of $La_{1/3}Ca_{2/3}MnO_3$. The white and colored stripes mean the regions of orbital-mixing angles corresponding to different MS.

4.4 $BiMnO_3$

The space symmetry of the compound is $C2/c$ [6] that is unusual for manganites. The possible OO is presented on Fig. 8 [10]. The OO of $BiMnO_3$ is caused not only by vibronic interaction of Mn^{3+} ion with local distortions of oxygen octahedra [10]. The non-local and non-linear vibronic terms could be taken into account as parameters:

$$\alpha_{1,n} = -|V_e|Q_{\theta,n} - \alpha_{\theta,n}; \alpha_{2,n} = -|V_e|Q_{\varepsilon,n} - \alpha_{\varepsilon,n}, \quad (17)$$

where n is Mn^{3+} sublattice number (n=1e, 2e, 1d, 2d).

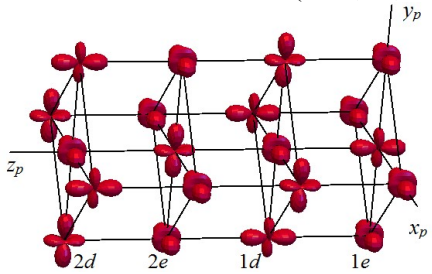

Fig.8. OO of $BiMnO_3$ in pseudoperovskite axes. Mn^{3+} ions as mixed single-electron e_g- functions are drawn. OO is drawn with respect of additional terms (16) in vibronic Hamiltonian (1) [10].

The main parts of coefficients could be estimated as $-|V_e|Q_{\theta,e}$=0.18 eV, $-|V_e|Q_{\varepsilon,e}$=–0.32 eV, $-|V_e|Q_{\theta,1d}$=0.10 eV, $-|V_e|Q_{\varepsilon,1d}$=0.32 eV, $-|V_e|Q_{\theta,2d}$=–0.36 eV, $-|V_e|Q_{\varepsilon,2d}$= –0.005 eV. The wave function of the Mn^{3+} sublattice is of the same form as in Eq. (11). There are two Mn^{3+} positions– 4e and 4d– with different local symmetry. OO with local symmetry account is described by correlation:

$$\Theta_1 = \Theta_2 = \Theta_e, \Theta_3 \approx -2\pi/3 - \Theta_4 = \Theta_d. \quad (18)$$

If $\alpha_{\theta,n}=\alpha_{\varepsilon,n}$ =0, it means only local linear vibronic interaction's influence. The orbital mixing angles are $\Theta_e = 300°, \Theta_d = 67°$. These values are inconsistent with found MS. However, the account of non-linear vibronic terms drastically changes the orbital states of d-position Mn^{3+} ions [10]. The superexchange interaction is of 1 type (Mn^{3+}–Mn^{3+}). As opposed to $LaMnO_3$, there are six different values of SE interaction.

The diagram of possible MS is drawn on Fig. 9. OO, caused by linear vibronic interaction (dark arrows on Fig. 9), leads to MS frustration in different directions (y_p or z_p). The possible structures are: G-type AFM without frustration, F-type FM structure, C-type AFM with FM chains approximately along x_p direction, A_1-type AFM with FM planes parallel to x_py_p-planes, A_2-type AFM with FM planes parallel to x_pz_p-planes. The regions of orbital mixing angles supporting the experimental F-type MS approximately are: $\Theta_e \approx 300^0$, $90 \le \Theta_d \le 160$.

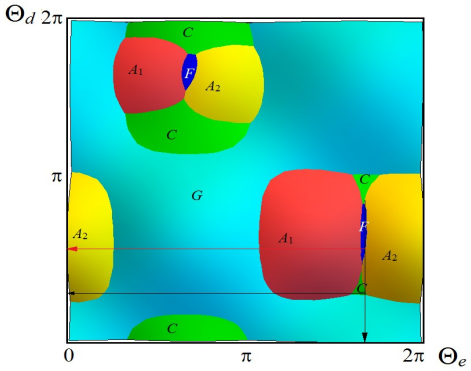

Fig. 9. Phase diagram of possible MS depending upon orbital mixing angles for $C2/c$ space group. Black arrows denote OO of Mn^{3+} sublattices in $BiMnO_3$ due to local linear vibronic interaction [10]. Red arrow shows possible orbital state for experimental [6] MS. A_1, A_2, C, G, F denote types of MS.

5 Conclusions

The uniform approach to description of orbital and magnetic structure of insulating manganite crystals is proposed. The model of orbital structure uses 2 parameters per Mn^{3+} position. For magnetic structure description – only 1 parameter per JT position is needed.

The support by Act 211 Government of the Russian Federation, contract № 02.A03.21.0006 is acknowledged.

References

1. J.B. Goodenough, Phys. Rev. **100**, 564 (1955); E.O Wollan, W.C. Koehler, Phys. Rev. **100**, 545 (1955).
2. T. Kimura *et al.*, Phys. Rev. B, **68**, 060403 (2003)
3. Y. Yamada *et al.*, Phys. Rev. Lett., **77**, 904 (1996).
4. M. Mochizuki, N. Furukawa, Phys. Rev B, **80**, 134416 (2008).
5. P. G. Radaelli *et al.*, Phys. Rev. B, **55**, 3015 (1997).
6. D.P. Kozlenko *et al.*, Phys. Rev. B, **82**, 014401 (2010).
7. I.V. Soloviev, S.A. Nikolaev, Phys. Rev. B **90**, 184425 (2014)
8. D.I. Khomskii *et al.*, JETP **122**, 484 (2016)
9. L.E. Gontchar, A.E. Nikiforov, Phys. Rev. B **66**, 014437 (2002)
10. L.E. Gonchar, A.E. Nikiforov, Phys. Rev B., **88**, 094401 (2013)
11. I.V. Soloviev, Phys. Rev. Lett., **91**, 177201 (2003)
12. V.I. Anisimov, AIP Conference Proc. **1297**, 3 (2010).
13. D. Nazipov et al., J of Phys.: Conf. Ser., **833,** 012006 (2017).
14. A.E. Nikiforov, S.E. Popov, Appl. Phys. A, **74**, 1743 (2002).
15. R. Kováčik *et al.*, Phys. Rev. B, **93**, 075139 (2016).
16. Beom Hyun Kim, B.I. Min, Phys. Rev. B, **80**, 064416 (2009).
17. L.E. Gontchar, A.E. Nikiforov, J. Magn. Magn. Mater., **300**, 167 (2006).
18. P.G. Radaelli *et al.*, Phys. Rev. B, **59**, 14440 (1999).